sensors

MDPI

Article

Estimating Pore Water Electrical Conductivity of Sandy Soil from Time Domain Reflectometry Records Using a Time-Varying Dynamic Linear Model

Basem Aljoumani [1,*] **, Jose A. Sanchez-Espigares** [2] **and Gerd Wessolek** [3]

[1]   Department of Ecology, Ecohydrology and Landscape Evaluation, Technische Universität Berlin
       Ernst-Reuter Platz 1, 10587 Berlin, Germany
[2]   Department of Statistical and Operational Research, Universitat Politècnica de Catalunya (UPC), Jordi
       Girona, 31, 08034 Barcelona, Spain; josep.a.sanchez@upc.edu
[3]   Department of Ecology, Technische Universität Berlin Ernst-Reuter Platz 1, 10587 Berlin, Germany;
       gerd.wessolek@tu-berlin.de
*   Correspondence: basem.aljoumani@tu-berlin.de

check for
updates

Abstract: Despite the importance of computing soil pore water electrical conductivity (σ_p) from soil bulk electrical conductivity (σ_b) in ecological and hydrological applications, a good method of doing so remains elusive. The Hilhorst concept offers a theoretical model describing a linear relationship between σ_b, and relative dielectric permittivity (ε_b) in moist soil. The reciprocal of pore water electrical conductivity ($1/\sigma_p$) appears as a slope of the Hilhorst model and the ordinary least squares (OLS) of this linear relationship yields a single estimate ($\widehat{1/\sigma_p}$) of the regression parameter vector (σ_p) for the entire data. This study was carried out on a sandy soil under laboratory conditions. We used a time-varying dynamic linear model (DLM) and the Kalman filter (Kf) to estimate the evolution of σ_p over time. A time series of the relative dielectric permittivity (ε_b) and σ_b of the soil were measured using time domain reflectometry (TDR) at different depths in a soil column to transform the deterministic Hilhorst model into a stochastic model and evaluate the linear relationship between ε_b and σ_b in order to capture deterministic changes to ($1/\sigma_p$). Applying the Hilhorst model, strong positive autocorrelations between the residuals could be found. By using and modifying them to DLM, the observed and modeled data of ε_b obtain a much better match and the estimated evolution of σ_p converged to its true value. Moreover, the offset of this linear relation varies for each soil depth.

Keywords: electrical conductivity; relative dielectric permittivity; time domain reflectometry; kalman filter; dynamic linear model

1. Introduction

Salinization reduces crop productivity, decreases profitability, and causes land scarcity [1]. Thus, it decreases the world's agricultural productivity and causes a global income loss of US\$ 12 billion per year [2]. Extracting soil solution by suction or using saturated paste conductivity measurements are the common methods to determine the electrical conductivity of soil pore water (σ_p) as an indicator of the soil salinity; however, they are labour- and cost intensive. There is no evidence that all ions are collected in the sample extract [3]. For soil salinity assessment, it is important to look for practical methods that evaluate the soil salinity state temporally and spatially. These methods help to correctly evaluate soil salinity evolution and reasonably predict its values [4–9]. In recent times, soil electromagnetic sensors have been used to estimate bulk electrical conductivity (σ_b). Then, methods are required to transform σ_b to σ_p [3,6,10].

According to Wyllie and Southwick [11], three conductance pathways, see Figure 1, contribute to the σ_b of a soil: (i) solid phase pathway through soil particles that are continuous contact with one another, (ii) liquid phase pathway through dissolved ions in the soil water inhabiting the large pores, and (iii) a liquid–solid interphase pathway through exchangeable cations like surfaces of clay minerals. Electrical conductivity (EC) in the liquid phase (σ_p) is used to estimate the soil salinity, a high EC refers to a high concentration of soluble salts, and vice versa. The σ_p could be estimated if the relationship between σ_p, σ_b, and water content (θ) is fixed [12–14]. The discovered linear correlation between the soil relative dielectric permittivity (ε_b) and σ_b values [15] enabled Hilhorst [3] to convert σ_b to σ_p by using a theoretical model. According to Hilhorst, σ_p can be determined from the equation:

$$\sigma_p = \frac{\varepsilon_p \sigma_b}{\varepsilon_b - \varepsilon_{\sigma_b=0}} \tag{1}$$

where σ_p is the pore water electrical conductivity (dS/m); ε_p is the relative dielectric permittivity of the soil pore water (dimensionless), ε_b is the relative dielectric permittivity of the bulk soil (dimensionless, relative dielectric permittivity is dimensionless since it is a ratio of permittivity of medium to the permittivity of free space), σ_b is the bulk electrical conductivity (dS/m), $\varepsilon_{\sigma b=0}$ is the relative dielectric permittivity of the soil when the bulk electrical conductivity is 0 (dimensionless). However, $\varepsilon_{\sigma b=0}$ appears as an offset of the linear relationship between ε_b and σ_b. The Hilhorst model [3] concluded that his method could be validated for water contents between 0.10 and saturation and for a conductivity of the pore water up to 0.3 S m^{-1}. He found that $\varepsilon_{\sigma b=0}$ depends on soil type and varies between 1.9 and 7.6. He recommended using 4.1 as a generic offset. Many studies applied the deterministic Hilhorst model [3] in their experiments to convert σ_b into σ_p but they did not use the same offset to achieve their study objective. For example, some studies concluded their work by using different offsets (within the range of 3.67 to 6.38) according to the soil type [10]. The producer of capacitance soil moisture sensors 5TE [16] recommends the use of an offset $\varepsilon_{\sigma b=0}$ of 6 while another study found that an offset $\varepsilon_{\sigma b=0}$ = 6 does not present a good linear relationship between ε_b and σ_b [17]. The WET sensor (Delta-T Device Ltd., Cambridge, UK) is a frequency domain dielectric sensor. It has been designed to estimate the σ_p based on the Hilhorst model [3] and incorporate the standard offset $\varepsilon_{\sigma b=0}$ = 4.1 of the model in the software of the device. By applying the Hilhorst model [3] in a saline gypsum-influenced soil, the accuracy of the WET sensor in predicting σ_p was very poor when using the offset model =4.1 [18]. Another study used a WET sensor for experimental measurements in the laboratory using four different soils (sand, sandy loam, loam, and clay) [9] and found that the offset depends on both soil type and σ_p, where it becomes larger for larger σ_p. Moreover, oscillator frequency and sensor circuitry could affect the estimation of ε_b and water content (θ) [19].
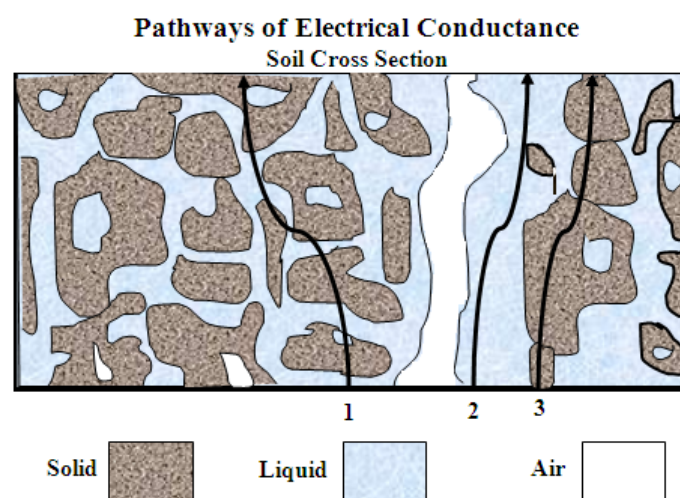
Figure 1. Three conductance pathways for the σ_b measurements, inspired by Wyllie and Southwick [11].

There are three elementary causes responsible for why the deterministic system and control theories do not produce a totally sufficient means of performing this analysis and design:

(i)　　many effects are left unknown since the objective of the model is to represent the main modes of system response,

(ii)　　deterministic models are driven not by only our own control inputs but also disturbances which we can neither control nor model deterministically, and

(iii)　　sensors do not offer exact readings of chosen quantities but present their own system dynamics and distortions as well and these devices are noise corrupted [20]. Despite the importance of computing σ_p from σ_b, a good method for doing so remains elusive (Campbell [16], personal communication).

Solute transport and water flow in the unsaturated zone are normally derived from the classical Richards equation and the convection–dispersion equations. Deterministic explanations of these equations are important aspects of research; due to soil heterogeneity at a variety of spatial scales, these equations for predicting actual field-scale processes are being increasingly questioned [21]. Therefore, some researchers working on soil heterogeneity concluded that for the evolution of soil water and solutes, it is more desirable to use stochastic models rather than constant values, where the parameters of stochastic transport models are treated as random variables with discrete values assigned according to a given probability distribution [21–26]. Among stochastic models, many studies used Kalman filtering in hydrological applications. A Kalman filter is an optimal recursive data processing algorithm that recursively couples the most recent measurements into the linear model to update the model state output [27]. Under the assumption that the linear system is a stochastic process with Gaussian noises, it produces the best estimation with minimum mean square error and it has been widely used in hydrological models to optimally merge information from the model simulations and the independent observations with appropriate modeling [28–32].

In previous work, we installed frequency domain reflectometry (FDR) sensors (5 TE), which are commercially available from METER Group, Inc. USA, in field conditions at different depths where the soil is heterogeneous to estimate σ_p [22]. We used ε_b and σ_b observations to modify the Hilhorst deterministic model [3] to a stochastic model using a time-varying dynamic linear model and Klaman filter before studying the linear relationship between them.

In this study, we used Time Domain Reflectometry (TDR) sensors (FP/mts), which are commercially available from Easy Test, Poland, to measure ε_b and σ_b in laboratory conditions where the soil is homogeneous. Then, we tried to use the Hilhorst model [3] to convert σ_b to σ_p. Later, we could show the weakness of applying the deterministic Hilhorst model [3] even in homogeneous soils. Thus, we are aiming to adapt this approach to a stochastic model under laboratory conditions. Thus, we used one homogeneous soil type to accurately estimate the changes in σ_p over time and to conclude whether the model offset is constant or if it changes in one soil profile.

2. Material and Methods

2.1. The Column Experiment

To achieve the objective of this study, we used two soil columns with a height of 55 cm provided by a sprinkler, see Figure 2. The lower boundary was controlled using a vacuum pump at a constant pressure head of −30 hPa. The columns were packed with a density of 1.4 g/cm^3. The substrate was sand, 80% of which was fine sand. The water content during packing was approximately 4 m^3/m^3. The TDR and soil temperatures sensors were installed in four depths: 7, 21, 35, and 48 cm. Since the soil is sand, the soil relative dielectric permittivity (ε_b), bulk electrical conductivity (σ_b), and temperature were measured every 5 min to obtain enough observations for modeling.
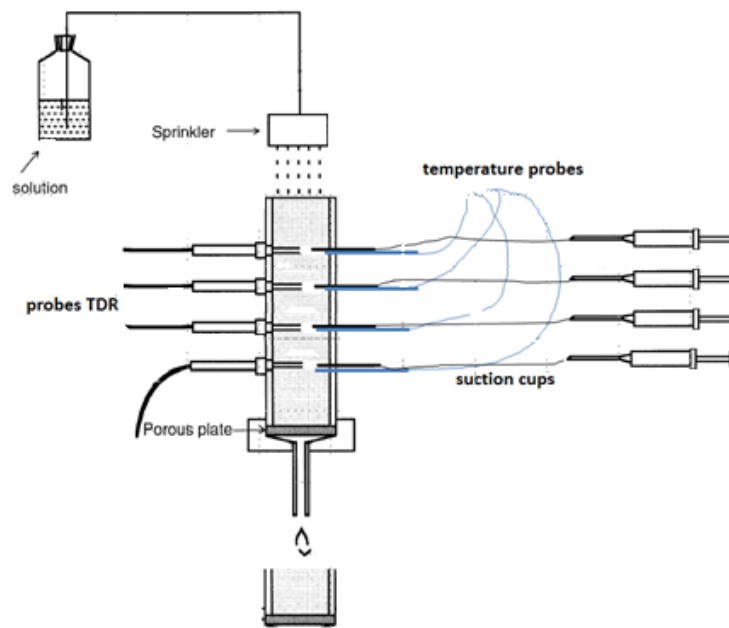
Figure 2. Measurement set.

Additionally, porous suction cups for taking soil solution samples were installed at each depth to validate the results of our model. The lower boundary of the column uses a membrane to let the water drain. Drainage water was collected in a bottle under -30 hPa vacuum, which is supplied in the range from -20 to -30 hPa. The sprinkler is 5 cm above the soil surface and allows water to drop through small nozzles. Five irrigation events using KCl solution with different electrical conductivities were applied. The first three events were irrigated with 20 dS/m of KCl, then the fourth, and fifth events with 30 dS/m of KCl. The flux was approximately 1 l/h. The columns were free of salt at the beginning and before the irrigations events started. The TDR probes are FP/mts commercially available from Easy Test, Poland, and have been calibrated in air and deionized water. The temperature probes are Thermistors of the type 2k252 (type Fenwal UUA 32J3) with a range of -20 up to 60 °C. Soil temperature data ($Tsoil$) were used to estimate the relative dielectric permittivity of the soil pore water directly (ε_p):

$$\varepsilon_p = 80.3 - 0.37(T_{soil} - 20) \tag{2}$$

To apply the dynamic linear model and the Kalman filter, a time series of the variable of interest is needed [27]. In our study, time series of ε_b, σ_b, and ε_p are required to estimate σ_p. Therefore, we used five irrigation events with two levels of KCL solution to obtain the variation of these variables over time for each depth. In total, 289 observations were made of σ_b, ε_p, and ε_b for each soil depth and these were used to estimate both the offset $\varepsilon_{\sigma b=0}$ of the modified Hilhorst model [3] and the evolution of σ_p at its corresponding depth, of which 144 observations were used to validate their forecasts.

2.2. Time-Varying Dynamic Linear Model

In general, the state space model is identified by two assumptions, (i) there is a hidden or latent process x_t called the state process. The state process is assumed to be a Markov process, where past and future values of x_t are independent, conditional on the present x_t, ($\{x_s, S > t\}$, and $\{x_s, S < t\}$ are independent on the x_t), (ii) the observations, y_t are independent given the states x_t. This means that the dependence among the observations is generated by states. The dynamic linear model (DLM) or linear Gaussian state space model, in its simple form, employs a first-order, p-dimensional vector autoregression as the state equation:

$$x_t = x_{t-1} + w_t \qquad w_t \sim \mathcal{N}(0, W_t) \tag{3}$$

We do not observe the state vector x_t directly, but only a linear transformed version of them with noise added, say:

$$y_t = A_t x_t + v_t \qquad v_t \sim \mathcal{N}(0, V_t) \tag{4}$$

y_t is an m-dimensional vector, representing the observation at time t, A_t is a $q \times p$ measurement or observation matrix. Equation (4) is called the observation equation, in which v_t, w_t are the Gaussian white-noise errors. The evolution variances are V_t, W_t and can be estimated from available data using maximum likelihood or Bayesian techniques.

In this study, we modified the deterministic Hihlorst model (1) to a stochastic one. The model (1) has the variables σ_b, ε_p, σ_p, ε_b, and $\varepsilon_{\sigma b=0}$. The σ_p and $\varepsilon_{\sigma b=0}$ are unobserved and they need to be estimated by the state Equation (3) as x_t, while σ_b, ε_p, and ε_b are observed by the sensors (ε_p is calculated from Equation (2) using soil temperature sensor data) and represented by observation Equation (4) as y_t.

The R [33] package, dlm [34], provides an integrated environment for Bayesian inference using DLM, and the package includes functions for Kalman filtering and smoothing, as well as for maximum likelihood estimation.

3. Results and Discussion

3.1. Deterministic Model

The offset of the Hilhorst model [3] can be calculated from Equation (1):

$$\varepsilon_b = (1/\sigma_p)\varepsilon_p \times \sigma_b + \varepsilon_{\sigma_b=0} \tag{5}$$

We derived the offset ($\varepsilon_{\sigma b=0}$) from this linear model after using measurements of ε_b and σ_b. For example, applying the ordinary least squares (OLS) on measurements of ε_b and σ_b obtained from soil column 2 data during the third irrigation at a depth of 21 cm, Table 1 shows that the offset of the linear relationship between ε_b–σ_b is 9.41. Further, the single estimate of the slope $(\widehat{1/\sigma_p})$ of the regression parameter vector $(1/\sigma_p)$ for the entire data set is very small. Thus, the estimated soil pore water electrical conductivity (σ_p) is too high compared with the EC meter value, see Table 2. Afterward, we applied the Durbin–Watson test in order to test if there was any autocorrelation between the residuals of the regression. Table 3 shows that there is an extremely strong and positive autocorrelation, meaning that the result of that regression is not valid.

Table 1. Estimated parameters gained from the linear regression analysis.

	Estimate	Std. Error	*t* Value	Pr (>|t|)
$\varepsilon_{\sigma b=0}$	9.411	8.591×10^{-3}	1095.4	$<2 \times 10^{-16}$ ***
$1/\sigma_p$	6.963×10^{-4}	4.461×10^{-6}	156.1	$<2 \times 10^{-16}$ ***

Significance: *** $p < 0.001$.

Table 2. Electrical conductivity of the soil solution (dS/m) according to soil column number, irrigation event, and depth (cm); it is collected by porous suction cups and measured by an electrical conductivity (EC) meter device.
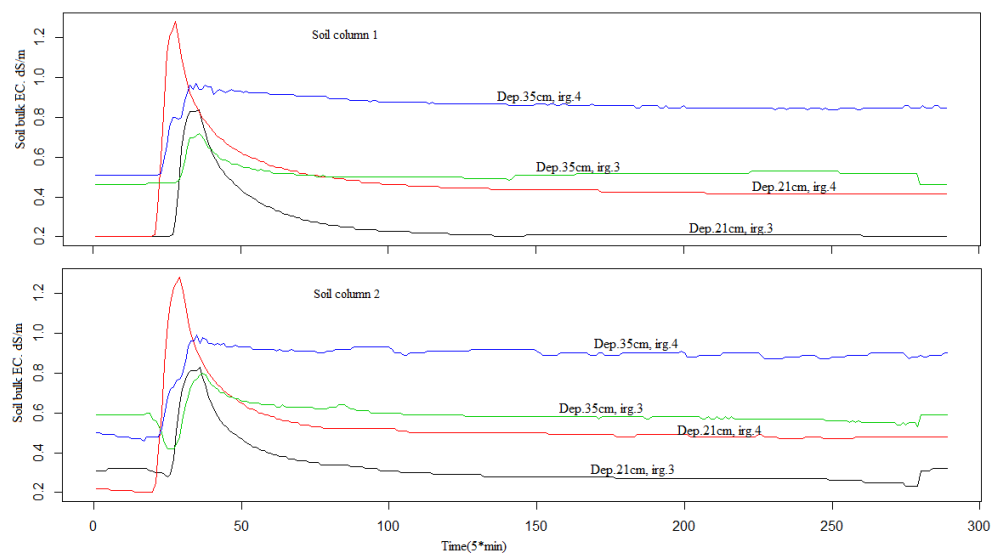
Soil Column 1				Soil Column 2			
Irrigation Event 3		Irrigation Event 4		Irrigation Event 3		Irrigation Event 4	
Depth: 21 cm	Depth: 35 cm	Depth: 21 cm	Depth: 35 cm	Depth: 21 cm	Depth: 35 cm	Depth: 21 cm	Depth: 35 cm
15.96	18	21.89	22.35	18.61	14.97	25.67	22

Table 3. Durbin–Watson test for linear regression ε_b-σ_b.

Lag	Autocorrelation	D-W Statistic	*p*-Value
1	0.852	0.278	0

For each irrigation event, we obtained one solution sample at each depth by using porous suction cups. Unfortunately, some samples did not have enough solution to measure their electrical conductivity using the EC meter device. Table 2 shows the values of EC measured by the EC meter device. The table shows eight EC values from the EC meter according to the depth and irrigation event number for each soil column. Due to the variability in the water flow in unsaturated soil, we observed in our experiment a variation in the time needed to collect the solution sample. More time was required to collect enough solution for the EC meter device when a greater number of ions gathered in the sample resulting in a high EC value of the sample. Therefore, there is a difference in the EC values between the soil columns at the same depth, see Table 2. We applied a modified Hilhorst model on the eight time-series data corresponding to Table 2 (depth, irrigation event, and soil column) to compare our finding of σ_p obtained from our modified model to the values of σ_p obtained by the EC meter device, see Table 2.

The reason for choosing 1 l/h for the irrigation rate and 5 min for the irrigation interval is visualized in Figure 3. At each depth, we could see how the bulk electrical conductivity responds to the irrigation event.

Figure 3. Bulk electrical conductivity (σ_b) in the two soil columns for two irrigation events (N°.3 and N° 4) at two depths (21 cm and 35 cm). Series peaks are related to time irrigation.

3.2. Time-Varying Linear Dynamic Model (LDM)

The deterministic Equation (5) can be modified into the time-varying DLM for observation and unobservable (state) models. In this case, the observation data are the soil relative dielectric permittivity (ε_b), bulk electrical conductivity (σ_b), and the relative dielectric permittivity (ε_p), while the unobservable data are the offset ($\varepsilon_{\sigma b=0}$) and pore water electrical conductivity (σ_p). Equation (4) can be modified to the time-varying DLM as follows:

- The observation equation can be obtained by modifying the Hilhorst model [3] (written in Equation (5)) into a stochastic equation, in accordance with Equation (4) as follows:

$$(\varepsilon_b)_t = \left(\varepsilon_{\sigma_b} = 0\right)_t + \left(\varepsilon_p * \sigma_b\right)_t \left(\frac{1}{\sigma_p}\right)_t + v_t$$
$$v_t \sim \mathcal{N}\left(0, \sigma_v{}^2\right)$$

(6)

- The state equation (unobservable data) in Equation (3) is $\varepsilon_{\sigma b = 0}$, and the slope, $1/\sigma_p$. They can be converted to the unobservable state equation of the time-varying DLM according to Equation (3). The unobservable state equation can be arranged as follows:

$$\begin{cases} (\varepsilon_{\sigma_b} = 0)_t = (\varepsilon_{\sigma_b} = 0)_{t-1} \\ \left(\frac{1}{\sigma_p}\right)_t = \left(\frac{1}{\sigma_p}\right)_{t-1} + w_t w_t \sim N(0, (\sigma_w)_t^2) \end{cases} \qquad (7)$$

Here, we consider $\varepsilon_{\sigma b = 0}$ as a constant. The actual value is related only to its past value. The slope $1/\sigma_p$ changes over time and its actual value is related to its past value plus the Gaussian white-noise errors (w_t). We applied the equation in reverse order to estimate the state variables ($\varepsilon_{\sigma b = 0}$ and σ_p) at all time points from a complete series of the soil relative dielectric permittivity (ε_b). This process is known as smoothing.

An example of the evolution of ε_b, ε_p, and σ_b data needed for the Hilhorst model [3] is shown in Figure 4. By applying the Equations (6) and (7) using DLM and the Kalman filter on the eight time-series data, we see in Figure 5 the observed and predicted time series of the soil relative dielectric permittivity (ε_b). The predicted and observed values of ε_b agree reasonably well. The mean absolute prediction error (MAPE) for the time series never exceeded 0.02.
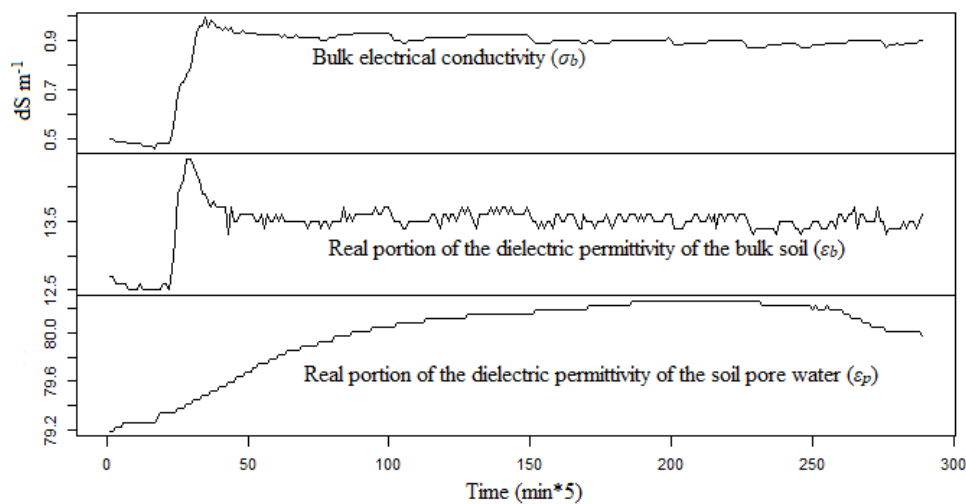

Figure 4. Known variables for the Hilhorst model (σ_b, ε_b, and ε_p); data from soil column 2, depth 35 cm and irrigation event N°4.

Since the prediction of the soil relative dielectric permittivity (ε_b) is valid, the estimation of the electrical conductivity of pore water (σ_p) and the offset $\varepsilon_{\sigma b = 0}$, see Equation (7), are also valid because they are used in the prediction of the soil relative dielectric permittivity (ε_b) and have converged to their true values. The evolution of σ_p over time obtained by DLM is presented in Figure 6; it shows the importance of using DLM because it obtained all the changes of σ_p over time and not a single value of σ_p for the entire data set. Another interesting aspect is that Figure 6 shows the changes in the model offset for each irrigation event at each depth. This finding is very important since it shows that the offset does not depend on the soil type [10,14–16] nor on the soil type and salinity [17] when two columns with the same type soil are used, as in this study. Moreover, in Figure 6 we put the corresponding value of σ_p measured by the EC meter device for each depth according the irrigation event and soil column number.

Comparing the mean evolution of σ_p values obtained from our modified Hilhorst model, see Figure 6, with the single corresponding EC value obtained from porous suction cups and measured by the EC meter device, see Table 2, we found that they agree very well ($R^2 = 72\%$).

From these results, three advantages are evident when using DLM and a Kalman filter to estimate σ_p in two homogenous soil columns; first, we observed that the offset value of the Hilhorst model does not depend on the soil type and σ_p and it changes in the same soil profile. Secondly, we obtained the changes in the estimated σ_p over time and not just a single value as a coefficient for the entire data set. Third, the estimated changes in σ_p occur instantly and save time and labor costs.
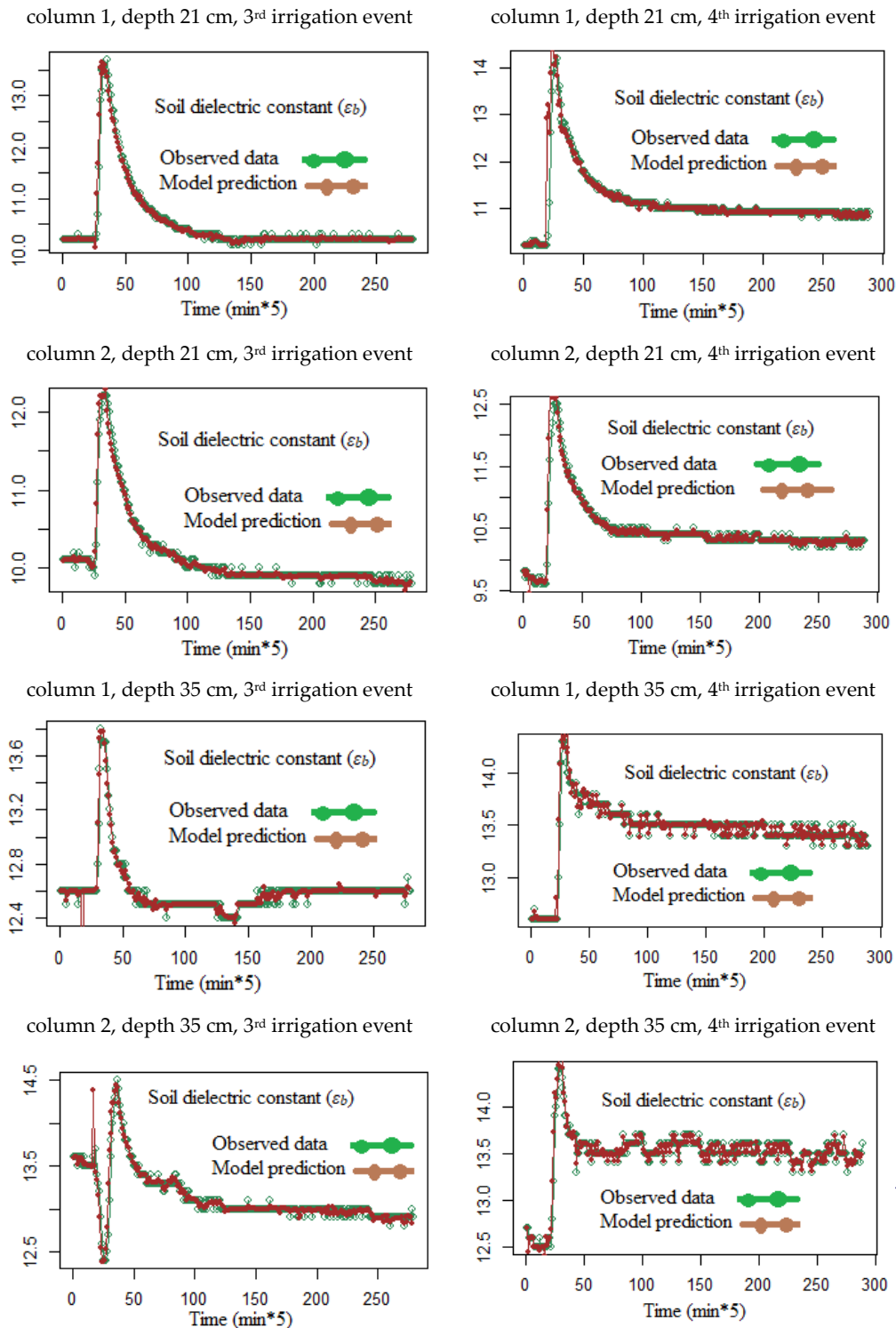
Figure 5. Observed and predicted soil relative dielectric permittivities according to the soil column number, depth, and irrigation event.
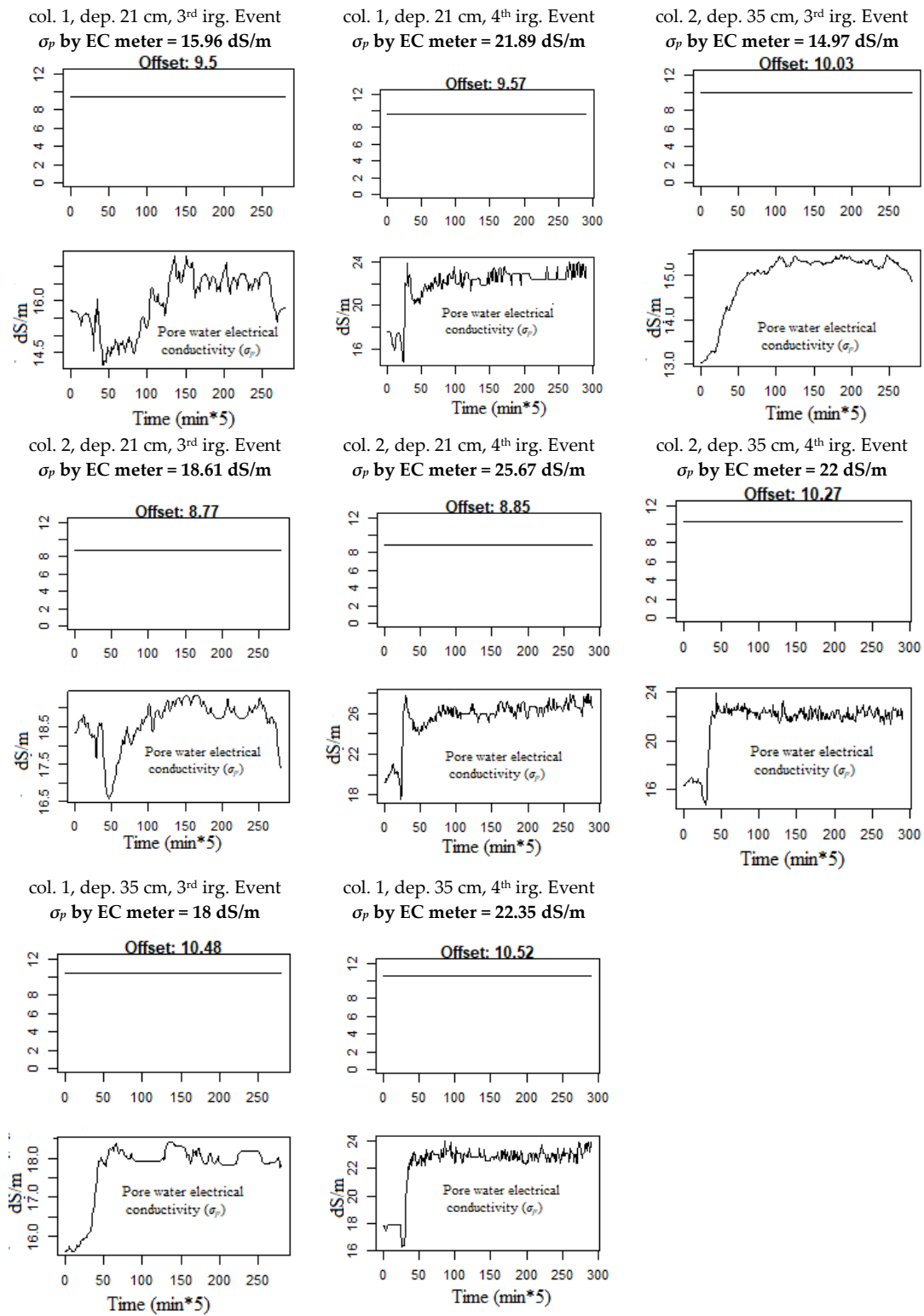
Figure 6. Estimation of the unobservable data ($\varepsilon_{\sigma b = 0}$ and σ_p) by applying the time-varying dynamic linear model (DLM) and the Kalman filter on the data according to the soil column number (col.), depth (dep.), and irrigation event (irg. Event), the corresponding of σ_p by EC meter device is given for each estimated σ_p.

4. Conclusions

In this study, we applied the ε_b-σ_b linear relationship to homogeneous soil column data obtained from TDR sensors. We found an extremely strong positive autocorrelation between the residuals of the regression analysis. When residuals are correlated, the least squares method is not the most efficient model coefficient estimator. By modifying the regression by a time-varying dynamic linear model (DLM), the match between the observed and modeled data of ε_b is significantly improved and the estimated evolution of σ_p converges to its true value. Moreover, in this study, we used two homogeneous soil columns with the same condition to show that the offset of the Hilhorst model [3] is not constant, as suggested for all moist soil or, as others suggested, that it is soil-type-dependent [10, 14–16] or soil-type- and salinity-dependent [17]. We repeated the experiment to show that the offset changes even in the same soil type and the same conditions. A dynamic linear model enables the capture of the offset changes and it shows the importance of calculating it simultaneously when estimating σ_p using the Hilhorst model. The next promising step would be programming and inserting these models into the TDR software in order to estimate the soil pore water electrical conductivity (σ_p) from senor records directly.

References

1. Thiruchelvam, S.; Pathmarajah, S. *An Economic Analysis of Salinity Problems in the Mahaweli River System H Irrigation Scheme in Sri Lanka*; EEPSEA: Ho Chi Minh, Vietnam, 1999; p. 47.
2. Ghassemi, F.; Jakeman, A.J.; Nix, H.A. *Salinisation of Land and Water Resources: Human Causes, Extent, Management and Case Studies*; CAB International: Wallingford, CT, USA, 1995.
3. Hilhorst, M.A. A Pore Water Conductivity Sensor. *Soil Sci. Soc. Am. J.* **2000**, *64*, 1922–1925. [CrossRef]
4. Hajrasuliha, S.; Baniabbassi, N.; Metthey, J.; Nielsen, D.R. Spatial Variability of Soil Sampling for Salinity Studies in Southwest Iran. *Irrig. Sci.* **1980**, *1*, 197–208. [CrossRef]
5. Cetin, M.; Kirda, C. Spatial and Temporal Changes of Soil Salinity in a Cotton Field Irrigated with Low-Quality Water. *J. Hydrol.* **2003**, *272*, 238–249. [CrossRef]
6. Rhoades, J.D; Shouse, P.J.; Alves, W.J.; Manteghi, N.A.; Lesch, S.M. Determining Soil Salinity from Soil Electrical Conductivity Using Different Models and Estimates. *Soil Sci. Soc. Am. J.* **1990**, *54*, 46–54. [CrossRef]
7. Shouse, P.J.; Goldberg, S.; Skaggs, T.H.; Soppe, R.W.O.; Ayars, J.E. Changes in Spatial and Temporal Variability of SAR Affected by Shallow Groundwater Management of an Irrigated Field, California. *Agric. Water Manag.* **2010**, *97*, 673–680. [CrossRef]
8. Li, X.; Yang, J.; Liu, M.; Liu, G.; Yu, M. Spatio-Temporal Changes of Soil Salinity in Arid Areas of South Xinjiang Using Electromagnetic Induction. *J. Integr. Agric.* **2012**, *11*, 1365–1376. [CrossRef]
9. Kargas, G.; Persson, M.; Kanelis, G.; Markopoulou, I.; Kerkides, P. Prediction of Soil Solution Electrical Conductivity by the Permittivity Corrected Linear Model Using a Dielectric Sensor. *J. Irrig. Drain. Eng.* **2017**, *143*, 04017030. [CrossRef]
10. Persson, M. Evaluating the Linear Dielectric Constant-Electrical Conductivity Model Using Time-Domain Reflectometry. *Hydrol. Sci. J.* **2002**, *47*, 269–277. [CrossRef]
11. Wyllie, M.R.J.; Southwick, P.F. An Experimental Investigation of the S.P. and Resistivity Phenomena in Dirty Sands. *J. Pet. Technol.* **1954**, *6*, 44–57. [CrossRef]
12. Rhoades, J.D.; Raats, P.A.C.; Prather, R.J. Effects of Liquid-Phase Electrical Conductivity, Water Content, and Surface Conductivity on Bulk Soil Electrical Conductivity[1]. *Soil Sci. Soc. Am. J.* **1976**, *40*, 651–655. [CrossRef]

13. Mualem, Y.; Friedman, S.P. Theoretical Prediction of Electrical Conductivity in Saturated and Unsaturated Soil. *Water Res. Res.* **1991**, *27*, 2771–2777. [CrossRef]

14. Malicki, M.A.; Walczak, R.T. Evaluating Soil Salinity Status from Bulk Electrical Conductivity and Permittivity. *Eur. J. Soil Sci.* **1999**, *50*, 505–514. [CrossRef]

15. Malicki, M.A.; Walczak, R.; Koch, S.; Fluhler, H. Determining Soil Salinity from Simultaneous Readings of Its Electrical Conductivity and Permittivity Using TDR. In Proceedings of the Symposium and Workshop on Time Domain Reflectometry in Environmental, Infrastructure, and Mining Applications, Evanston, IL, USA, 7–9 September 1994; Volume 101, pp. 7–9.

16. Decagon Devices. *5TE Water Content, EC, and Temperature Sensors Operator's Manual*; Decagon Devices: Pullman, WA, USA, 2008.

17. Rodriguez, A.; Ruben, F. Calibrating Capacitance Sensors to Estimate Water Content, Matric Potential, and Electrical Conductivity in Soilless Substrates. Master's Thesis, University of Maryland, College Park, MD, USA, 2009.

18. Bouksila, F.; Persson, M.; Berndtsson, R.; Bahri, A. Soil Water Content and Salinity Determination Using Different Dielectric Methods in Saline Gypsiferous Soil/Détermination de La Teneur En Eau et de La Salinité de Sols Salins Gypseux à l'aide de Différentes Méthodes Diélectriques. *Hydrol. Sci. J.* **2008**, *53*, 253–265. [CrossRef]

19. Visconti, F.; Martínez, D.; Molina, M.J.; Ingelmo, F.; Miguel de Paz, J. A Combined Equation to Estimate the Soil Pore-Water Electrical Conductivity: Calibration with the WET and 5TE Sensors. *Soil Res.* **2014**, *52*, 419–430. [CrossRef]

20. Maybeck, P.S. *Stochastic Models, Estimation, and Control*; Academic Press: Cambridge, MA, USA, 1982.

21. Genuchten, M.V. Recent Progress in Modelling Water Flow and Chemical Transport in the Unsaturated Zone. In Proceedings of the 20th General Assembly of the International Union of Geodesy and Geophysics, Vienna, Austria, 11–24 August 1991; pp. 169–183.

22. Aljoumani, B.; Sànchez-Espigares, J.A.; Cañameras, N.; Wessolek, G.; Josa, R. Transfer Function and Time Series Outlier Analysis: Modelling Soil Salinity in Loamy Sand Soil by Including the Influences of Irrigation Management and Soil Temperature. *Irrig. Drain.* **2018**, *67*, 282–294. [CrossRef]

23. Aljoumani, B.; Sànchez-Espigares, J.A.; Cañameras, N.; Josa, R. An Advanced Process for Evaluating a Linear Dielectric Constant–Bulk Electrical Conductivity Model Using a Capacitance Sensor in Field Conditions. *Hydrol. Sci. J.* **2015**, *60*, 1828–1839. [CrossRef]

24. Aljoumani, B.; Sànchez-Espigares, J.A.; Cañameras, N.; Josa, R.; Monserrat, J. Time Series Outlier and Intervention Analysis: Irrigation Management Influences on Soil Water Content in Silty Loam Soil. *Agric. Water Manag.* **2012**, *111*, 105–114. [CrossRef]

25. Beven, K.; Germann, P. Macropores and Water Flow in Soils. *Water Res. Res.* **1982**, *18*, 1311–1325. [CrossRef]

26. White, R.E. The Influence of Macropores on the Transport of Dissolved and Suspended Matter Through Soil. In *Advances in Soil Science*; Stewart, B.A., Ed.; Springer: New York, NY, USA, 1985; pp. 95–120.

27. Kalman, R.E. A New Approach to Linear Filtering and Prediction Problems. *J. Basic Eng.* **1960**, *82*, 35–45. [CrossRef]

28. Wendroth, O.; Rogasik, H.; Koszinski, S.; Ritsema, C.J.; Dekker, L.W.; Nielsen, D.R. State-space Prediction of field-scale Soil Water Content Time Series in a Sandy Loam. *Soil Tillage Res.* **1999**, *9*, 85–93. [CrossRef]

29. Hoeben, R.; Troch, P.A. Assimilation of Active Microwave Observation Data for Soil Moisture Profile Estimation. *Water Resour. Res.* **2000**, *36*, 2805–2819. [CrossRef]

30. Moradkhani, H.; Sorooshian, S.; Gupta, H.V.; Houser, P.R. Dual State–Parameter Estimation of Hydrological Models Using Ensemble Kalman Filter. *Adv. Water Resour.* **2005**, *28*, 135–147. [CrossRef]

31. Anderson, J.L. An Ensemble Adjustment Kalman Filter for Data Assimilation. *Mon. Weather Rev.* **2001**, *129*, 2884–2903. [CrossRef]

32. Liu, Y.; Weerts, A.H.; Clark, M.; Hendricks Franssen, H.-J.; Kumar, S.; Moradkhani, H.; Seo, D.-J.; Schwanenberg, D.; Smith, P.; van Dijk, A.I.J.M.; et al. Advancing Data Assimilation in Operational Hydrologic Forecasting: Progresses, Challenges, and Emerging Opportunities. *Hydrol. Earth Syst. Sci.* **2012**, *16*, 3863–3887. [CrossRef]

33. R Core Team. *R: A Language and Environment for Statistical Computing*; R Foundation for Statistical Computing: Vienna, Austria, 2013.

34. Petris, G. An R Package for Dynamic Linear Models. *J. Stat. Softw.* **2010**, *36*. [CrossRef]